

# Rayleigh scattering and laser spot elongation problems at ALFA

E. Viard (eviard@eso.org), F. Delplancke (fdelplan@eso.org)  
and N. Hubin (nhubin@eso.org)  
*European Southern Observatory, Garching, Germany*

N. Ageorges (nancy@epona.physics.ucg.ie)  
*Physics Department, National University of Ireland, Galway, Ireland*

R. Davies (davies@mpe.mpg.de)  
*Max-Planck-Institut für extraterrestrische Physik, Garching, Germany*

## Abstract.

This paper describes the qualitative effects of LGS spot elongation and Rayleigh scattering on ALFA wavefront sensor images. An analytical model of Rayleigh scattering and a numerical model of laser plume generation at the altitude of the Na-layer were developed. These models, integrated into a general AO simulation, provide the sensor sub-aperture images. It is shown that the centroid measurement accuracy is affected by these phenomena. The simulation was made both for the ALFA system and for the VLT Nasmyth Adaptive Optics System (NAOS).

**Keywords:** adaptive optics, laser guide star, Rayleigh scattering, spot elongation

**Abbreviations:** NGS – Natural Guide Star; LGS – Laser Guide Star; AO – Adaptive Optics; FWHM – Full Width Half Maximum;

## 1. Introduction

In LGS-AO systems, many issues have to be studied and tested on real hardware and the ALFA system in Calar Alto is a remarkable test bench for the characterization and improvement of LGS-AO operation. In Shack-Hartmann systems, it can be observed that the laser spot shape, as seen from different wavefront sensor sub-apertures, varies as a function of the launching telescope position relative to the sensor. The spot shape depends on 2 phenomena :

1. the Na-layer thickness : producing a 3-D laser plume of about 10 km which is seen from different angles by the different wavefront sensor sub-apertures and leads to different laser spot elongations for each sub-aperture ;
2. the presence of Rayleigh scattering in the lower atmosphere : which gives a cone of light below the laser plume itself ; the Rayleigh cone can be seen



by the sensor sub-apertures under certain circumstances to be studied here.

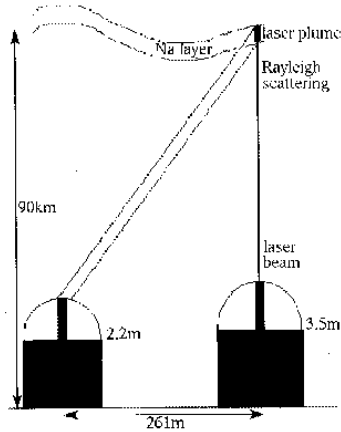


Figure 1. Calar Alto set-up

We have modeled both phenomena independently. Then to calibrate and verify these theoretical and analytical models a common observation programme was conducted (in August 1998) at Calar Alto. The Na plume elongation and the Rayleigh cone due to the ALFA laser beam were observed from the neighboring 2.2 m telescope. The experimental results (Delplancke et al., 1998) were used to constraint the models, as well as to study the evolving Na layer density profile. The experimental set-up is shown in figure 1.

The models were introduced into a general AO software package, also developed in the frame of the LGS network, to get the wavefront sensor sub-aperture images and the corresponding centroid positions in any experimental conditions. We have computed the Rayleigh scattering and the Na spot as seen from wavefront sensor sub-apertures, both in the ALFA case and in the case of a 8-m telescope (typically the Nasmyth Adaptive Optics System - NAOS-of the ESO Very Large Telescope project).

The influence of the LGS shape on the wavefront sensor performances and on noise propagation in the AO system can be evaluated. The modal optimization of the AO closed loop can be adapted accordingly for optimal results, based on noise propagation. This technique must then be compared with other proposed ways of removing the perspective elongation effects (Beckers, 1992).

Here are presented the modeling principles, their correlations with observations, and the qualitative results (sections 2 for the Rayleigh scattering, and 3 for the spot elongation) as well as a first analysis of the LGS shape influence on measurement noise in section 4.

## 2. Rayleigh scattering modeling

The Calar Alto experiment was modeled using analytical Rayleigh single scattering theory and geometrical optics.

The hypotheses made in the modeling are the following :

- the geometry is as shown in Fig. 2 with a Na-layer altitude of 90 km.

- the scattering is only due to Rayleigh scatterers (of size  $\ll$  than the wavelength), air molecules were used. We did not take the aerosols into account for 2 reasons : first, their concentration is highly variable with the period of the year, with the observatory location, and with the local weather, making the modeling very difficult. Moreover, as we are interested in the top of the Rayleigh cone close to the Na-layer, it corresponds to high altitudes where there are few aerosols.
- we considered only single scattering.
- we neglected the loss of power of the laser beam due to the scattering when it is going up in the atmosphere (in case of pure Rayleigh scattering, this loss is lower than 1% on a path length of 100 km).
- the beam is supposed to have a constant width all along its path. Indeed, even if the beam is focalised on the Na-layer, its diameter does not change significantly due to the turbulence which is widening the spot. This was verified during Calar Alto run where the laser plume was observed to have a FWHM diameter of about 1 m (for a launched beam of 0.25 m).
- the beam is assumed wide enough to be resolved by the wavefront sensor camera on several pixels. Again, it was verified during last August observations.
- the laser launch telescope has no central obscuration.
- we neglected the influence of the beam polarization because we are working in backscattering where the scattered light polarization is identical to the propagating beam one.
- the atmospheric density model as a function of the altitude is the USSA-1962 model (McCartney, 1976a) whose profile is given in Fig.2.
- the Rayleigh scattering analytical formula is the classical one (van de Hulst, 1981) (McCartney, 1976b) :

$$\frac{dI_1(\alpha)}{d\Omega} = P_0 4 \pi^2 \frac{(n_0 - 1)^2}{N_0^2 \lambda^4} (\cos(\phi)^2 \cos(\alpha)^2 + \sin(\phi)^2) \quad (1)$$

where  $\frac{dI_1(\alpha)}{d\Omega}$  is the intensity of the light scattered by a single particle, per unit of solid angle  $\Omega$  in the direction  $\alpha$  (close to  $180^\circ$  in backscattering),  $P_0$  the power of the incident light per unit of surface,  $n_0$  the atmospheric refractive index at sea level (=1.000292),  $N_0$  the number of particles (molecules) per unit of volume at sea level(= $2.5 \times 10^{25}$  particles per cubic meter),  $\lambda$  the wavelength,  $\phi$  the angle between the scattering plane and the direction of polarization of the incident light.

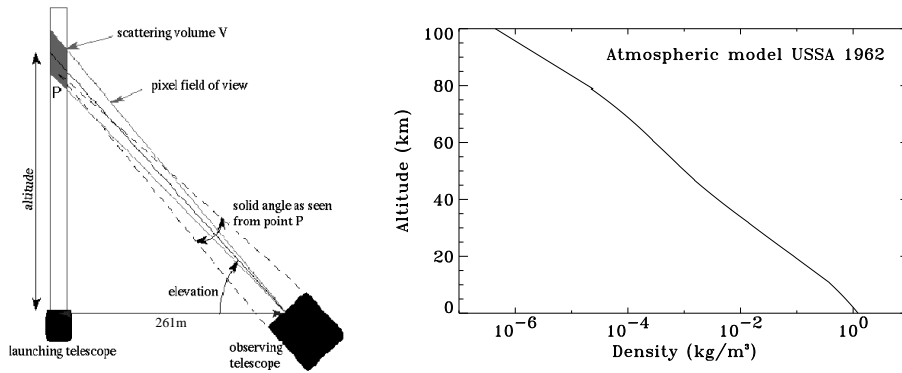


Figure 2. Left : Geometry used for the simulation. Right : Atmospheric density (in  $kg/m^3$ , in log-scale) as a function of the altitude (in km) as given by the model USSA-1962.

The model predicts correctly the presence of a maximum in intensity per pixel at a certain elevation depending mainly on the distance between the launching and observing telescopes, as observed during Calar Alto observation run from a telescope placed at 261 m from the launching one. This results from 3 effects :

- the decrease in atmospheric density with the altitude,
- the increase of the scattering volume (corresponding to one camera pixel, with the telescope elevation) and
- the increase of the distance between that volume and the observing telescope.



Figure 3. Na layer plume (right side) and Rayleigh cone top (just seen at the left side) as seen from the 2.2 m telescope (top) and as modeled (bottom). The image size is  $600 \times 80 \text{ arcsec}^2$ . Images are in linear scale

The model gives the right shape and the right intensity ratio between the Na plume (set, in the model, to a cumulated magnitude of 9, as observed from ALFA (Quirrenbach et al., 1997)) and the top of the Rayleigh cone as seen in figure 3.

The simulation gives also results comparable with images taken with the tv-guider camera of the 3.5 m telescope in Calar Alto (Fig. 4). The tv-guider

camera is much closer to the laser launch telescope and corresponds more to the close configuration encountered with the wavefront sensor.

The simulation helps us to predict that the elevation of the apparent intensity maximum increases when the observing telescope gets closer to the launching one; the top of the Rayleigh cone approaches the Na-layer LGS. For close configurations (separation between the launching telescope and the observing sub-aperture lower than 1 m), the top of the Rayleigh cone can even apparently *touch* the Na plume.

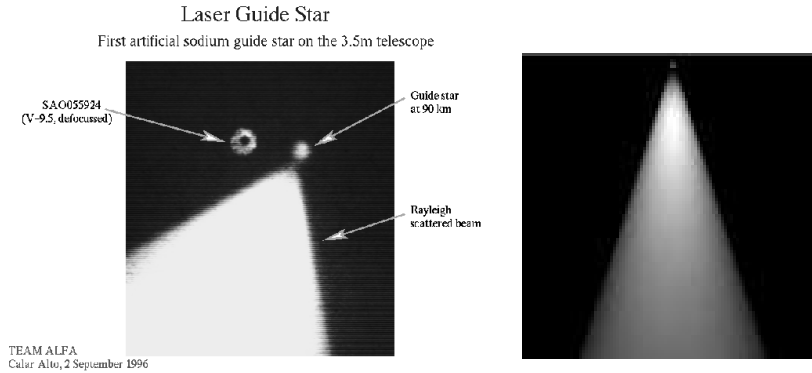


*Figure 4.* Comparison between ALFA off-axis tv-guider image of the LGS and Rayleigh cone (left) and the image obtained with the simulation (right) for the same scale and field of view. Distance tv-guider - launch telescope = 1 m. LGS magnitude = 7. Output laser power = 2.2 W. Pixel size = 0.37 arcsec

### 3. Sodium layer spot modeling

The Na layer spot simulation is divided into 3 steps whose parameters are the following :

- the launch of the laser beam by a telescope of adjustable diameter (here set to 0.25 m in ALFA case), without central obscuration. The beam is supposed gaussian, its waist (related to the full width half max) was chosen here equal to 33 % of the diameter, its focalization was set on the Na-layer supposed to be at 90 km altitude, and its power was set to 2 W continuous.
- the upward conical propagation of the laser beam through a von Kármán atmosphere (here with  $r_0 = 20 \text{ cm}$  and  $L_0 = 20 \text{ m}$ ) made of several layers (here 2 layers at 10 m and 10 km respectively). Fraunhofer propagation (Born and Wolf, 1959) is assumed here taking into account the focalization on the Na-layer.

- the generation of the 3-D spot in the Na-layer by computing the intensity pattern at different levels in this layer (supposed of FWHM equal to 7 km centered around an altitude of 90 km), supposing a gaussian distribution of the Na column density as a function of the altitude, and not considering saturation (because of the use of a continuous laser). The resonant backscattered number of photons is computed following the results obtained by Gardner (1989). The principle scheme of such a simulation is given in Fig. 5. An example of the so obtained 3D spot shape, as seen from the ground, is given in figure 6.

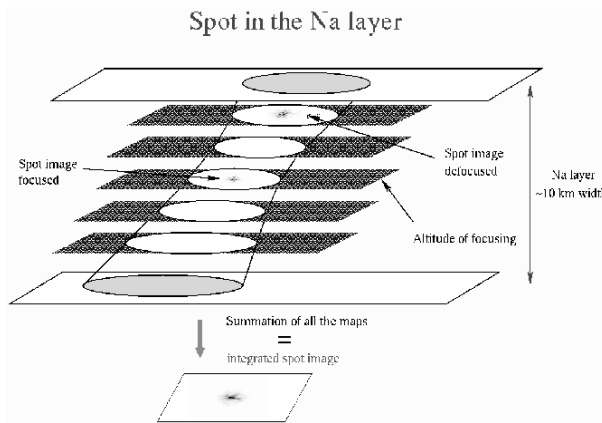


*Figure 5.* Principle scheme for the generation of the 3-D spot in the Na-layer. The sub-layer images are given for a 8-metre launching telescope in order to show the speckle due to the propagation through the turbulent atmosphere.

#### 4. Influence on Shack-Hartmann wavefront sensor performances

##### 4.1. RAYLEIGH CONE

As shown by the simulation and by the Calar Alto experiments, the Rayleigh cone intensity per pixel angularly close to the Na layer spot, increases when the observing aperture gets closer to the laser launching telescope. It will be the most important for the closest wavefront sensor sub-apertures in a LGS AO system. This situation was modeled both for ALFA (5x5 hexagonal sensor) and NAOS (14x14 square sensor) systems, considering that the minimum distance between sub-aperture and launching telescope is equal to 1 m. The results of such simulation are shown in figures 7 and 8.

In ALFA case, the Rayleigh cone is very important in the sub-aperture, closest to the laser launch. The total intensity due to the Rayleigh on the sub-aperture field of view is of the same order of magnitude as the total

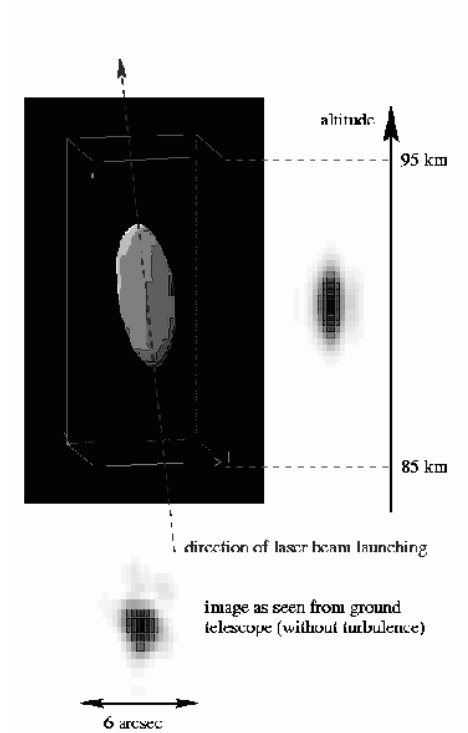


Figure 6. Example of a 3-D Na spot obtained with a 0.25 m launched beam, a 7 km FWHM Na layer at 90 km mean altitude, and a slightly off-axis launching direction.

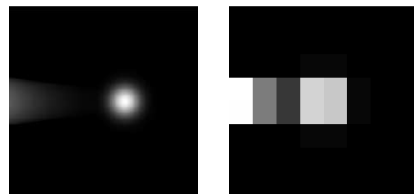


Figure 7. Rayleigh cone and Na spot images in a sub-aperture of ALFA. The Na spot has a global 9 magnitude, for a 2 W laser power. The 0.7 diameter sub-aperture center is located 1 m from the laser launching telescope. At left, the pixel size is equal to 0.023 arcsec while at right, the image is rebinned to the actual ALFA pixel size of 0.75 arcsec. The sub-aperture field of view is in both cases of 6 arcsec. The atmospheric turbulence is not taken into account. Laser launch telescope diameter = 0.25 m.

Na spot intensity. As the Rayleigh is situated only on one side of the Na spot, it is inducing a large bias on the centroid measurement. Fortunately it is not so affecting the other sub-apertures : for a laser-sub-aperture distance of 1.7 m, the Rayleigh total intensity is reduced to about 8 % of the Na spot total intensity.

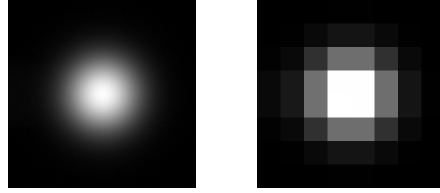


Figure 8. Rayleigh cone and Na spot images in a sub-aperture of NAOS (14x14). The Na spot has a global 9 magnitude, for a 2 W laser power. The 0.57 diameter sub-aperture center is located 1 m from the laser launching telescope. At left, the pixel size is equal to 0.009 arcsec while at right, the image is computed for the actual NAOS pixel size of 0.29 arcsec. The sub-aperture field of view is in both cases of 2.32 arcsec. The atmospheric turbulence is not taken into account. Laser launch telescope diameter = 0.25 m.

A solution to remove the Rayleigh scattering cone is to take the sub-aperture images with a detuned laser so that only the Rayleigh cone can be seen. This reference image is then subtracted from the real closed loop image before getting the centroid. It only works when the laser is launched from the center of the telescope so that the configuration is centrally symmetric. Indeed, if the laser is launched sidewise, the pupil rotation on the Shack-Hartmann sensor will induce a displacement of the laser launch position relative to the Shack-Hartmann axes. The Rayleigh cone aspect on each sub-aperture will vary with time and no easy calibration is possible. On the contrary, when the laser is centrally launched, the pupil rotation does not induce this displacement and the Rayleigh cone aspect (orientation and shape) remains the same at any moment (as long as the Rayleigh is constant). Still, the Rayleigh added noise has to be taken into account. This parasitic noise is of the order of  $5 e^-$  per pixel per ms, at his highest point. This is not negligible relative to the other noise sources : read-out noise (around  $6 e^-$  rms) and sky background noise. The Rayleigh cone can also be reduced by windowing the sub-aperture field of view and by temporal filtering in case of pulsed laser. Other means will be investigated, e.g. using the beam polarization properties.

On the contrary, Fig. 8 shows that the Rayleigh cone can be neglected in the case of NAOS. This is due to the fact that, in NAOS, the pixel scale is much smaller than in ALFA (0.29 arcsec versus 0.75 arcsec). The sub-aperture field of view is thus smaller, providing a kind of spatial filtering. Moreover, in NAOS, the Rayleigh cone is distributed on a larger number of pixels than in ALFA while the Na spot is not *diluted* so much. The intensity per pixel due to the Rayleigh scattering goes down to 4 % of the Na spot intensity per pixel. This represent a parasitic noise, after Rayleigh cone subtraction, of  $0.4 e^-$  per pixel per ms, which is negligible relative to the read-out noise.



## 4.2. SPOT ELONGATION

The 3-dimensional Na spot image, obtained as described the section 3, is then used in the wavefront sensor image computation.

Again Fraunhofer and weak fluctuations approximations are used : the scintillation is neglected and we propagate only phase variations through the same atmosphere as used in upward propagation, taking the cone effect into account. Phase at the entrance of the telescope is obtained and Shack-Hartmann wavefront sensor sub-aperture images are computed using Fourier optics :

- the 2-D Na spot source maps are obtained by projecting the 3-D map on each sub-aperture taking the perspective effects into account ;
- the sensor point-source images are computed by Fourier transform of the phase on the sub-apertures ;
- the convolution of the point-source images with the 2-D Na spot maps gives us the final sensor images.

This simulation was made in 2 cases : ALFA (3.5 m telescope with a 5x5 hexagonal Shack-Hartmann wavefront sensor) and NAOS (8 m telescope with a 7x7 square Shack-Hartmann sensor).

The 2-D Na spot maps are shown in Fig. 9 for ALFA and in Fig. 10 for NAOS and for different positions of the laser launch telescope relative to the pupil. The differential elongation of the spots as a function of the sub-aperture can be easily seen on the extracted contour plots. It is more noticeable with the 8 m telescope than with the 3.5 m.

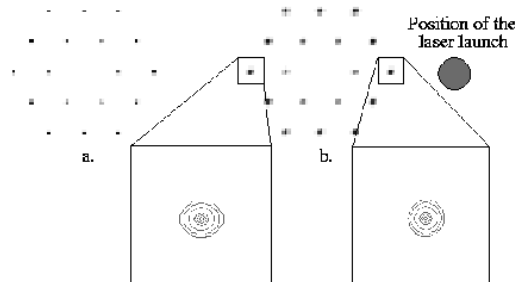


*Figure 9.* Right : Na spot elongation on the various sub-apertures of ALFA system (5x5 hexagonal array). The laser is launched from the pupil side (grey dot). The closest and farthest spots are enlarged as contour plots in order to show the differential spot elongation. The global field of view of the contour plots is 3 arcsec. It can be compared with the natural guide star spot shape (at left).

The spot elongation modifies the accuracy of the centroid measurement along its long axis. As the spot elongation is not the same for each sensor

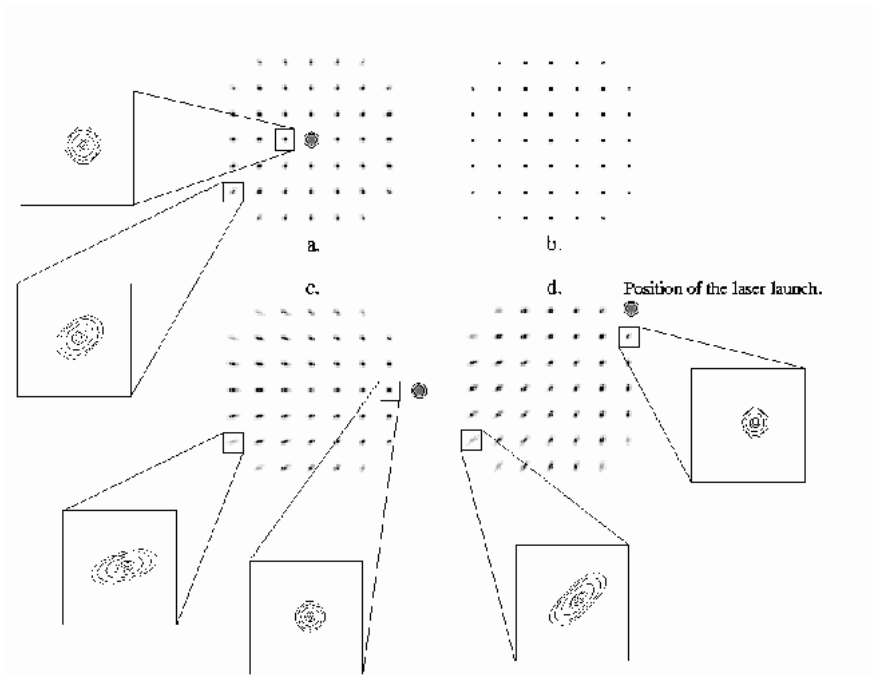


*Figure 10.* Na spot elongation on the various sub-apertures of NAOS system (8 m telescope, 7x7 square array) for various positions of the laser launch telescope (grey dot) : a) behind the secondary mirror, c) at the pupil side, along one of the sensor axes, d) at the pupil side and at 45° from the axes. It can be compared with the natural guide star spot shape (b). Some of the spots are enlarged into contour plots whose global field of view is 3 arcsec.

sub-apertures and as a function of the laser position, the noise on the centroiding measurement is different and therefore the noise propagation into the reconstructed modes is affected. This effect is negligible for ALFA. Indeed the measurement noises (read-out noise, background noise ...) are very large relative to the LGS signal and the laser spots are deformed due to atmospheric turbulence. The very slight spot elongation shown in figure 9 without noise nor perturbation is so completely dominated by other ALFA noise sources in real situations.

On the contrary, in system like NAOS where the measurement noises are considerably reduced, the spot elongation will have to be taken into account and the laser launch telescope position well chosen. Indeed, in an alt-azimutal telescopes, the pupil rotates on the sensor and if the launching laser is not located behind the telescope secondary mirror (central position), the shape of the spots on each sub-aperture will vary with time. This effect is well shown in Fig. 10 c and d.

In LGS AO operation, the differential noise propagation must be compensated via the reconstruction matrix and via an adapted modal optimization

in the time and mode filtering. If the spot elongation on one sub-aperture varies with time (i.e. with a lateral launching telescope), various reconstruction matrix have to be implemented as a function of the pupil position on the Shack-Hartmann sensor. The quantitative effects of these phenomenon on the adaptive optics loop performances have to be evaluated.

## 5. Conclusion and Perspectives

Experiments were conducted in Calar Alto with the 2.2 and 3.5 m telescopes and with ALFA, in order to study the Rayleigh scattering induced by the laser beam, and the spot elongation due to the non-negligible Na-layer thickness. The observations allowed us to develop and calibrate models of these phenomena. The models have been used to study the impact of Rayleigh scattering and spot elongation on the Shack-Hartmann wavefront sensor image and on the centroiding performances. The spot elongation was shown to be negligible in ALFA case while it is more important with an 8 m telescope. On the contrary, the presence of the top of the Rayleigh scattering cone appeared to be more noticeable in ALFA case and to induce a non-negligible bias in the centroiding measurements close to the laser launch telescope.

We are planning to make new observations in Calar Alto to exactly calibrate the photon returns from the Na spot and from the Rayleigh cone, together with Lidar measurements of the atmosphere. These data will be used to certify our developed models.

We will also test the polarization method for suppressing the Rayleigh cone in the sub-aperture images. Finally, the investigation of noise propagation in the AO loop with spot elongation will be pursued quantitatively. We plan to propose strategies to correct for this effect.

## Acknowledgements

This work is being performed in the frame of the ‘Laser Guide Star for 8-m Class Telescopes’ network of the European Commission *Training and Mobility of Researchers* programme (Contract no. FMRX-CT96-0094). The present research was a collaboration between the Max-Planck-Institut für extraterrestrische Physik in Garching, the European Southern Observatory and the National University of Ireland-Galway.

Special thanks go to the ALFA team (W. Hackenberg, M. Kasper, Th. Ott and S. Rabien) and the operators (J. Aceituno and L. Montoya) for their essential help with the laser.

## References

- Beckers, J.: 1992, 'Removing perspective elongation effects in Laser Guide Stars and their use in the ESO Very Large Telescope'. *Proceedings of ESO conference on Progress in Telescope and Instrumentation Technologies (April 27-30, 1992, Garching, Germany)* pp. 505–514.
- Born, M. and E. Wolf: 1959, *Principles of Optics*, pp. 381–385. Pergamon Press (London).
- Delplancke, F., N. Ageorges, N. Hubin, and C. O'Sullivan: 1998, 'LGS light pollution investigation in Calar-Alto'. In: *Proceedings of ESO-OSA Conference on Astronomy with Adaptive Optics (April 7-11, 1998, Sonthofen, Germany)*. pp. 501–512.
- Gardner, C.: 1989, 'Sodium resonance fluorescence Lidar applications in atmospheric science and astronomy'. In: *Proceedings of IEEE*, Vol. 77. pp. 408–418.
- McCartney, E.: 1976a, *Optics of the Atmosphere - Scattering by Molecules and Particles*, pp. 81–86. John Wiley & Sons (New York).
- McCartney, E.: 1976b, *Optics of the Atmosphere - Scattering by Molecules and Particles*, Chapt. 4. John Wiley & Sons (New York).
- Quirrenbach, A., W. Hackenberg, H. Holstenberg, and N. Wilnhammer: 1997, 'The Sodium Laser Guide Star System of ALFA'. In: *Proceedings SPIE in Adaptive Optics & Applications*, Vol. 3126. pp. 35–43.
- van de Hulst, H.: 1981, *Light scattering by small particles*, p. 65. Dover Publications (New York).